Electronic Supplementary Material (ESI) for CrystEngComm.

Assembling Photoactive Materials from Polycyclic Aromatic Hydrocarbons (PAHs): Room Temperature Phosphorescence and Excimer-Emission in Co-Crystals with 1,4-Diiodotetrafluorobenzene

Alessandra Azzali,[a] Simone d'Agostino,[a] Mattia Capacci,[a] Floriana Spinelli,[a] Barbara Ventura,*[b] and Fabrizia Grepioni*[a]

[a] Dipartimento di Chimica "Giacomo Ciamician", Università di Bologna, Via F. Selmi, 2, 40126 Bologna, Italy

[b] Istituto ISOF-CNR, Via P. Gobetti, 101, 40219 Bologna, Italy

ELECTRONIC SUPPORTING INFORMATION (8 pages)

Synthesis

Table ESI-1. Amounts of reagents used in the synthesis of the co-crystals A·$(I2F4)_2$, MA·I2F4, and $(MA)_4$·I2F4. A = anthracene, MA =9-methylanthracene, and I2F4 = 1,4-diiodotetrafluorobenzene.

PAH	(mg / mmol)	I2F4 (mg /mmol)	Stoichiometric Ratio	Outcome
A	62 / 0.35	140 / 0.35	1:1	A·$(I2F4)_2$ + A
A	96 / 0.50	100 / 0.25	2:1	A·$(I2F4)_2$ + A
A	37 /0.21	170 / 0.42	1:2	A·$(I2F4)_2$
MA	67 / 0.34	140 / 0.34	1:1	MA·I2F4
MA	36 / 0.18	150 / 0.37	1:2	MA·I2F4 + I2F4
MA	95 / 0.49	100 / 0.25	2:1	$(MA)_4$·I2F4 + MA + MA·I2F4
MA	119 / 0.61	90 / 0.22	3:1	$(MA)_4$·I2F4 + MA + MA·I2F4
MA	133 / 0.69	70 / 0.17	4:1	$(MA)_4$·I2F4

Ortep Drawings

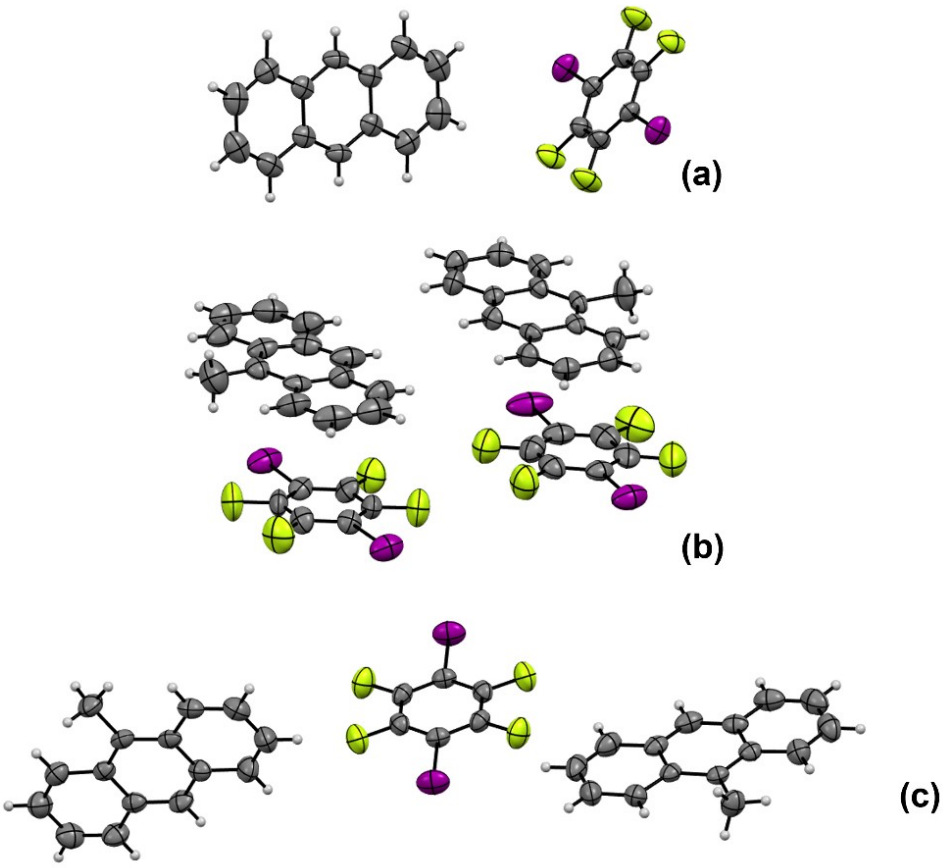

Figure ESI-1. ORTEP plots of the co-crystals (a) A·$(I2F4)_2$, (b) MA·I2F4, and (c) $(MA)_4$·I2F4. All the non-hydrogen atoms are represented by their 50% probability ellipsoids.

Powder X-ray Diffraction patterns

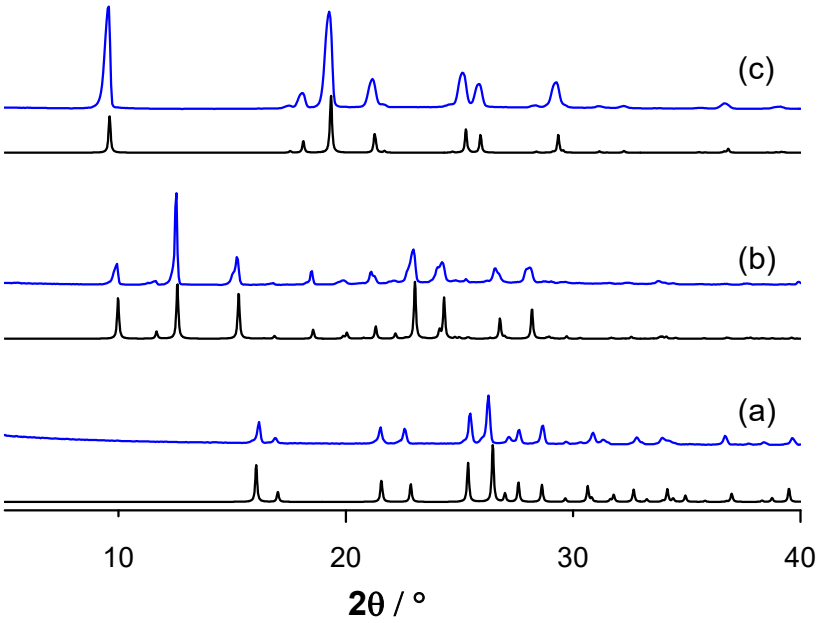

Figure ESI-2. Powder XRD patterns comparison between experimental (blue lines) and calculated on the basis of single crystal data retrieved from the CSD (black lines): (a) 1,4-diiodotetrafluorobenzene (refcode ZZZAVM02), (b) methylanthracene (refcode MANTHR01), and (c) anthracene (refcode ANTCEN).

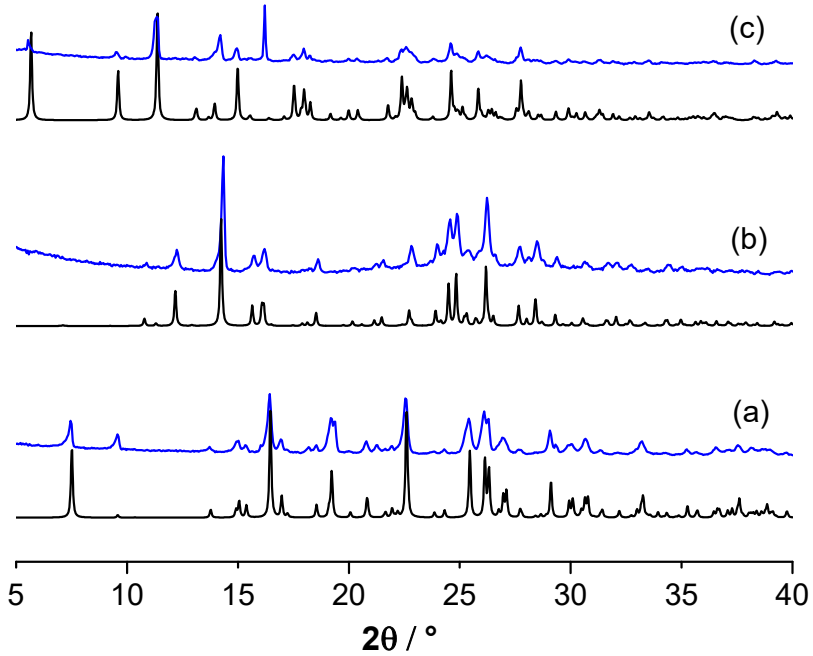

Figure ESI-3. Powder XRD patterns comparison between experimental (blue lines) and calculated on the basis of single crystal data from this work (black lines): (a) A·$(I2F4)_2$, (b) MA·I2F4, and (c) $(MA)_4$·I2F4.

Thermal gravimetric analysis (TGA)

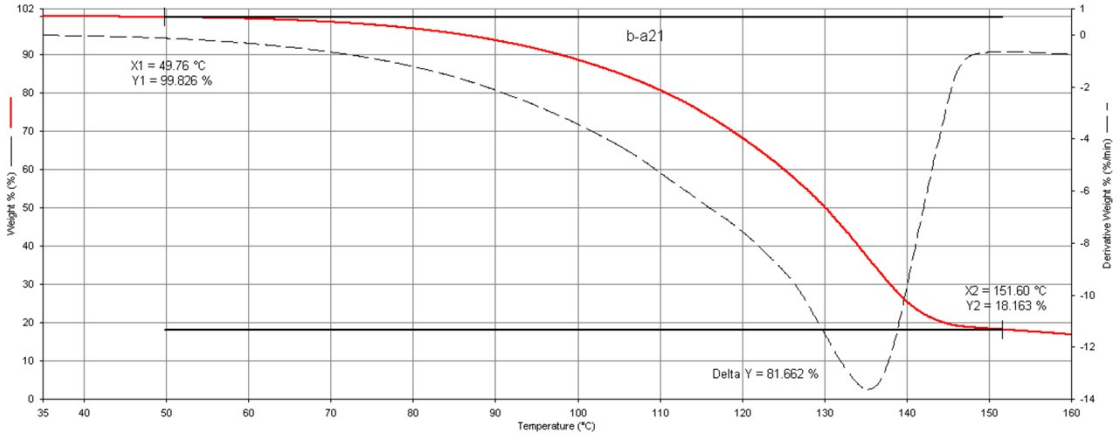

Figure ESI-4. Thermogram of A·(I2F4)$_2$.

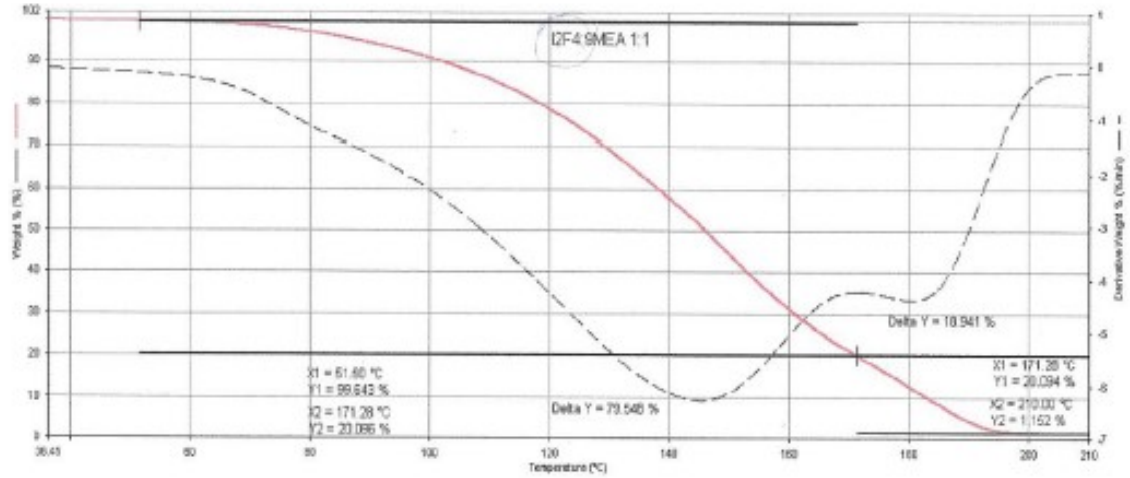

Figure ESI-5. Thermogram of MA·I2F4.

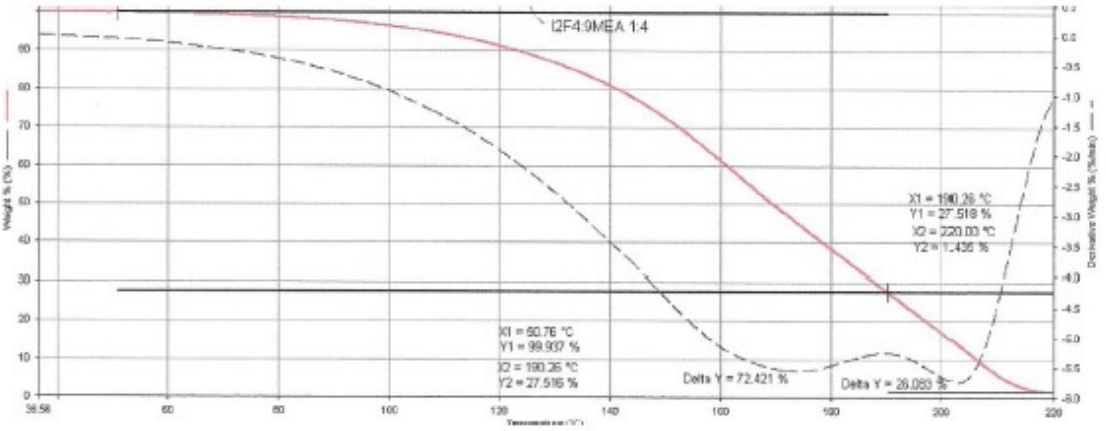

Figure ESI-6. Thermogram of (MA)$_4$·I2F4.

Photodimerization of crystalline MA

100 mg of pure methylanthracene (MA), previously recrystallized from ethanol, was irradiated under a 365 nm LED for ca 5 h. The so-obtained solid was subjected to powder XRD analysis and further identified as the head-to-tail 9-methylanthracene photodimer[1] (see Figure ESI-8).

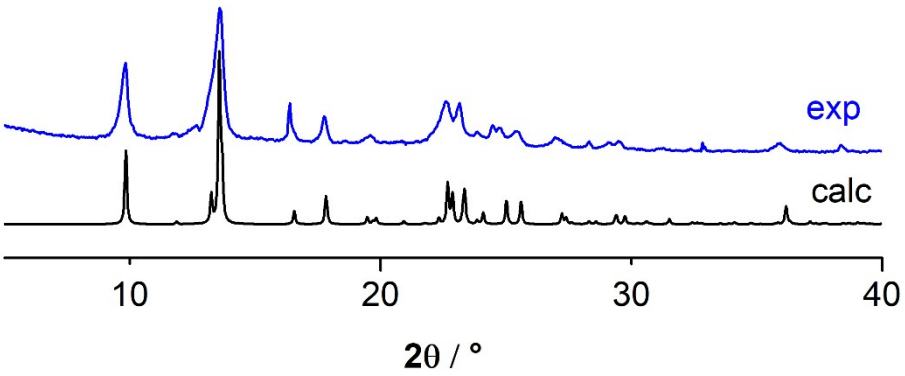

Figure ESI-7. Powder XRD pattern comparison between experimental (blue line) obtained after irradiation and calculated one based on the crystal structure retrieved from the CSD (black line) and corresponding to the photodimer (refcode QQQFES04).

NMR spectra

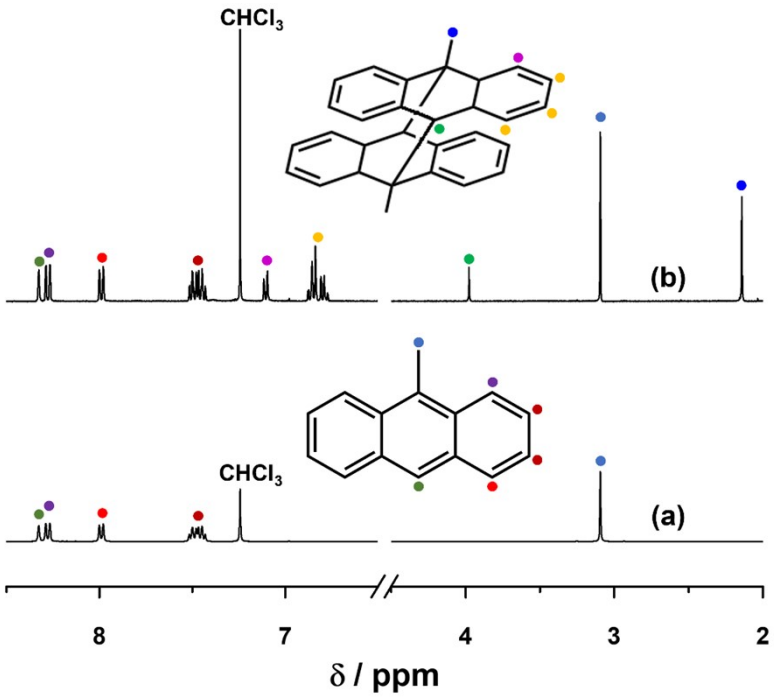

Figure ESI-8. ^{1}H-NMR spectra in $CDCl_3$ of the co-crystal $(MA)_4$·I2F4 before (a) and after irradiation (b).

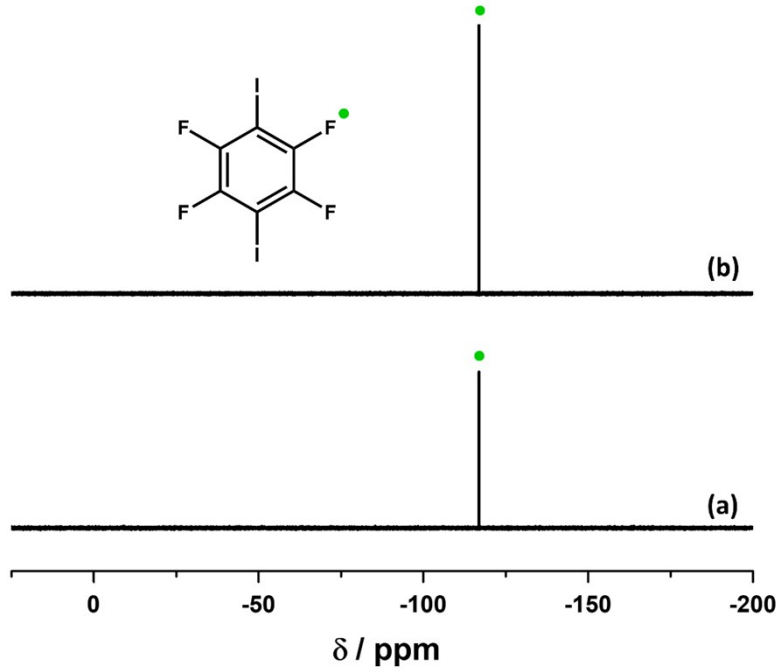

Figure ESI-9. ^{19}F-NMR spectra in $CDCl_3$ of the co-crystal $(MA)_4$·I2F4 before (a) and after irradiation (b).

Absorption, emission and excitation spectra of A, A·(I2F4)$_2$, MA, MA·I2F4, and (MA)$_4$·I2F4

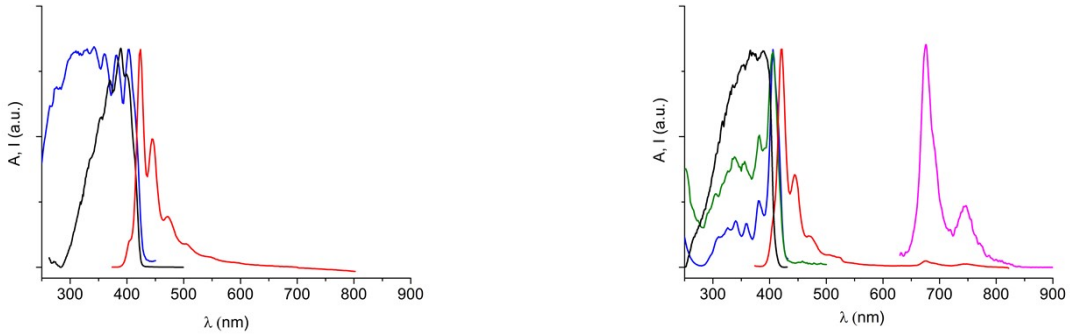

Figure ESI-10: Normalized absorption (black), emission (red, λ_{exc}= 360 nm) and excitation (blue, λ_{em}= 472 nm) spectra of A (left) and absorption (black), fluorescence (red, λ_{exc}= 360 nm), phosphorescence (pink, λ_{exc}= 380 nm) and excitation (blue, λ_{em}= 472 nm, fluorescence mode; green, λ_{em} = 700 nm, phosphorescence mode) spectra of A·(I2F4)$_2$ (right).

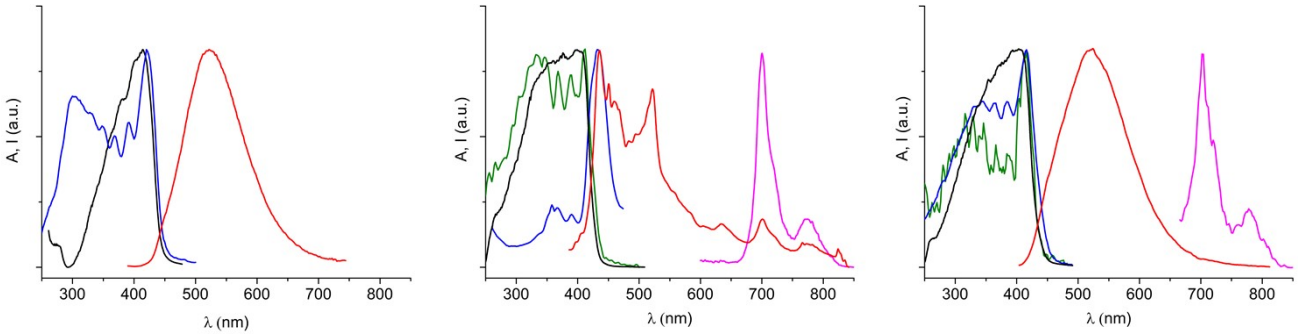

Figure ESI-11: Normalized absorption (black), emission (red, λ_{exc}= 380 nm) and excitation (blue, λ_{em}= 520 nm) spectra of MA (left); absorption (black), fluorescence (red, λ_{exc}= 360 nm), phosphorescence (pink, λ_{exc}= 380 nm) and excitation (blue, λ_{em}= 520 nm, fluorescence mode; green, λ_{em} = 700 nm, phosphorescence mode) spectra of MA·I2F4 (middle) and absorption (black), fluorescence (red, λ_{exc}= 360 nm), phosphorescence (pink, λ_{exc}= 380 nm) and excitation (blue, λ_{em}= 520 nm, fluorescence mode; green, λ_{em} = 700 nm, phosphorescence mode) spectra of (MA)$_4$·I2F4 (right).

Excited state lifetimes

Fluorescence lifetimes, detected by means of a single-photon counting apparatus, are reported in Table ESI-2 for MA, MA·I2F4 and $(MA)_4$·I2F4. In case of A and A·$(I2F4)_2$, measured fluorescence lifetimes were in the order of few nanoseconds, but the detection of longer lifetimes in the low energy region of the spectrum prompted us to perform a time-resolved luminescence analysis. Two components of the order of 1 ns and 6 ns characterize the fluorescence spectrum of A in the 400-470 nm region, while a third minor component with a longer lifetime of 109 ns is observable in the region 470-560 nm (Figure ESI-12). In the emission of A·$(I2F4)_2$ two main components of the order of 0.2 ns and 3 ns are accompanied by a small fraction of a longer component (550 ns) in the low energy region. Fluorescence decays at selected wavelengths in the two regions (420 nm and 470 nm) are reported in Figure ESI-13 for a visual comparison. The presence of two main components in both materials can be due to different environments experienced by the units in the crystals, both fluorescence lifetimes are indeed reduced in the co-crystal due to the increased intersystem crossing rate. The longer-lived emission can be tentatively ascribed to the presence of ground-state interactions between the PAHs units in the crystals.[2,3]

Table ESI-2: Fluorescence lifetimes of MA, MA·I2F4 and $(MA)_4$·I2F4 at room temperature in the solid-state (in brackets: fractional intensities); excitation at 370 nm.

	τ (ns)
MA	27.3 (30%), 61.5 (70%)
MA·I2F4	5.6
$(MA)_4$·I2F4	6.3 (60%), 35.7 (40%)

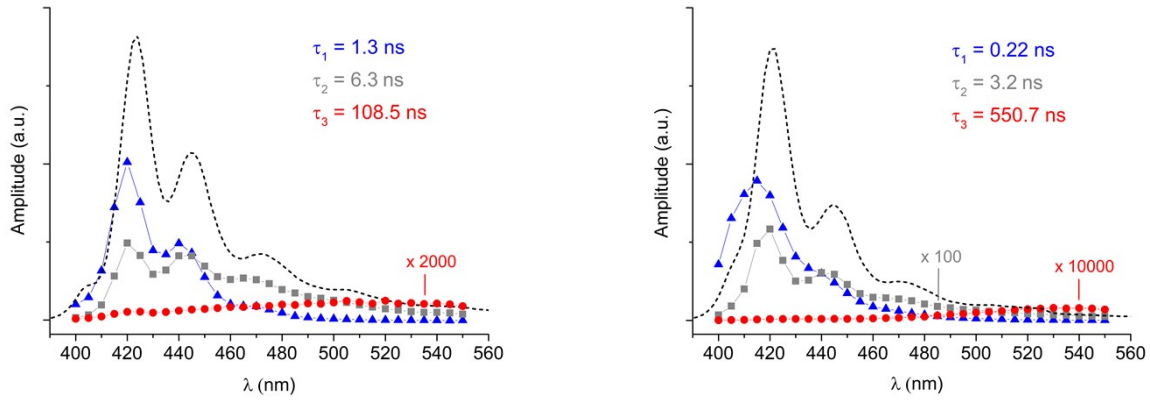

Figure ESI-12. DAS from time-resolved luminescence of A (left) and A·$(I2F4)_2$ (right) in the solid-state. The arbitrarily scaled steady-state emission spectrum (dashed black line) is reported for comparison purposes; the relevant lifetime components are indicated in the legend. In the graphs are shown the multiplication factors employed for some amplitudes.

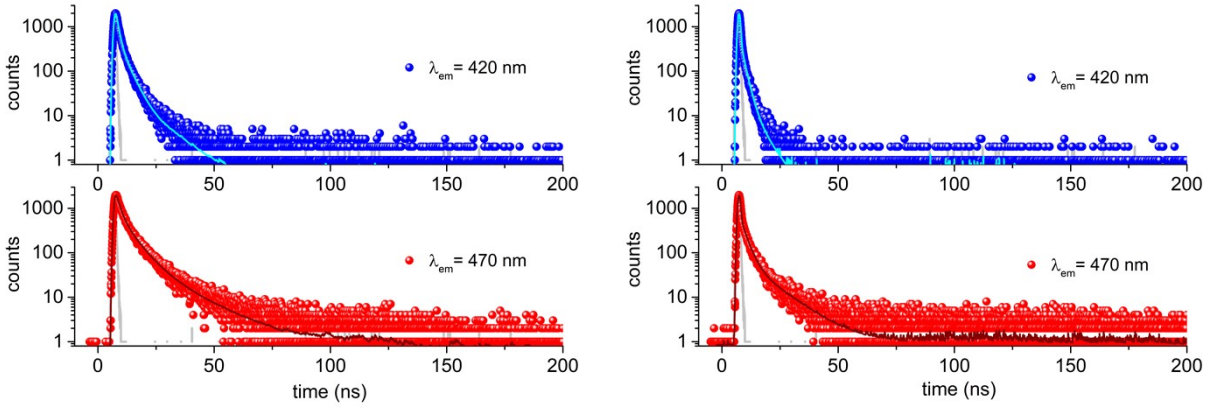

Figure ESI-13. Fluorescence decays, in logarithmic scale, of A (left) and A·(I2F4)$_2$ (right) in the solid state, collected at the indicated wavelengths. The excitation profiles are shown in light grey (λ_{exc}= 368 nm). The fittings are reported as lines.

Phosphorescence lifetimes, collected by means of a single-photon counting apparatus are reported in Table ESI-3.

Table ESI-3: Phosphorescence lifetimes of A·(I2F4)$_2$, MA·I2F4 and (MA)$_4$·I2F4 at room temperature in the solid-state (in brackets: fractional intensities); excitation at 370 nm.

	τ (μs)
A·(I2F4)$_2$	35.0 (15%), 280.6 (85%)
MA·I2F4	33.6 (20%); 200.7 (80%)
(MA)$_4$·I2F4	88.2 (25%); 322.2 (75%)

Intermolecular Interaction Energies

Interaction energies, resulting from the sum of electrostatic, polarization, dispersion and repulsion contributions, were evaluated with the help of the program CrystalExplorer (see references in the main text). Values for the three structures described in the paper are reported in the tables below.

Total interaction energies between pairs of molecules are indicated by the same colour in the table and in the corresponding figure (dashed lines).

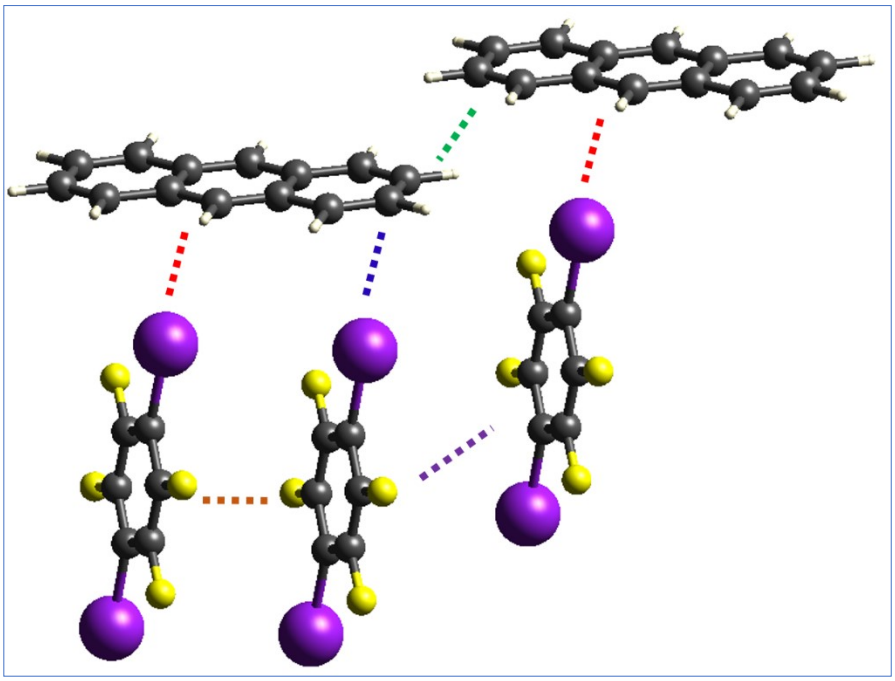

Figure ESI-14. Pairs of molecules contributing most to the total interaction energy in crystalline A·$(I2F4)_2$.

Table ESI-4. Electrostatic, polarization, dispersion, repulsion terms and total interaction energy within the pairs of molecules shown in Figure ESI-14. Evaluated with the Crystal Explorer Package and using the CE-HF/3-21G (k_ele = 1.019; k_pol = 0.651; k_disp =0.901; k_rep = 0.811) as energy model and basis set.[4-6]

Interaction	$E_{ELECTROSTATIC}$	$E_{POLARIZATION}$	$E_{DISPERSION}$	$E_{REPUSLSION}$	E_{TOTAL}
	-8.9	-2.0	-20.5	12.5	-18.8
	-12.5	-2.4	-20.5	22.2	-14.8
	-4.8	-0.8	-11.9	6.4	-10.9
	-3.3	-1.0	-39.7	18.8	-24.6
	-5.6	-0.6	-30.3	17.0	-19.7

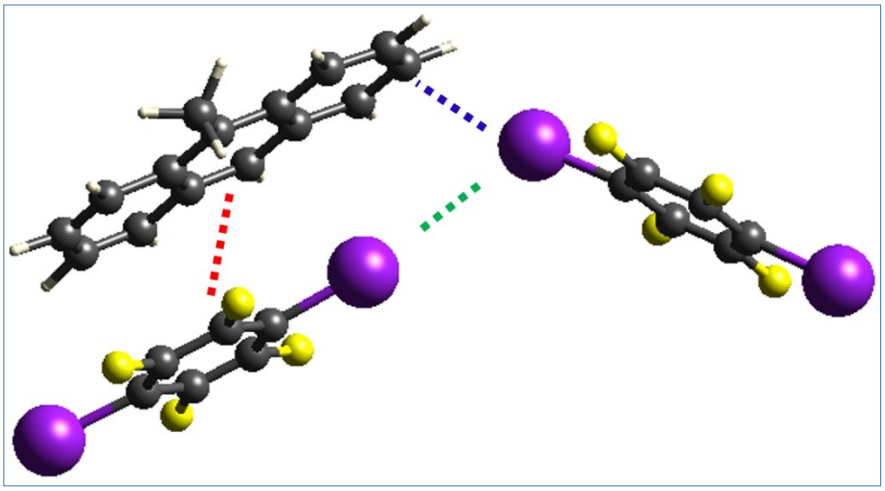

Figure ESI-15. Pairs of molecules contributing most to the total interaction energy in crystalline MA·I2F4.

Table ESI-5 Electrostatic, polarization, dispersion, repulsion terms and total interaction energy within the pairs of molecules shown in Figure ESI-15. Evaluated with the Crystal Explorer Package and using the CE-HF/3-21G (k_ele = 1.019; k_pol = 0.651; k_disp =0.901; k_rep = 0.811) as energy model and basis set.[4-6]

	Interaction	$E_{ELECTROSTATIC}$	$E_{POLARIZATION}$	$E_{DISPERSION}$	$E_{REPUSLSION}$	E_{TOTAL}
Pair 1		-15.4	-3.4	-56.6	32.4	-42.6
		-6.4	-1.3	-11.7	9.1	-10.6
		-1.9	-0.4	-7.1	5.7	-4.0
Pair 2		-17.7	-3.7	-58.7	34.4	-45.4
		-5.4	-1.1	-10.7	6.4	-10.7
		-2.2	-0.4	-7.4	6.8	-3.7

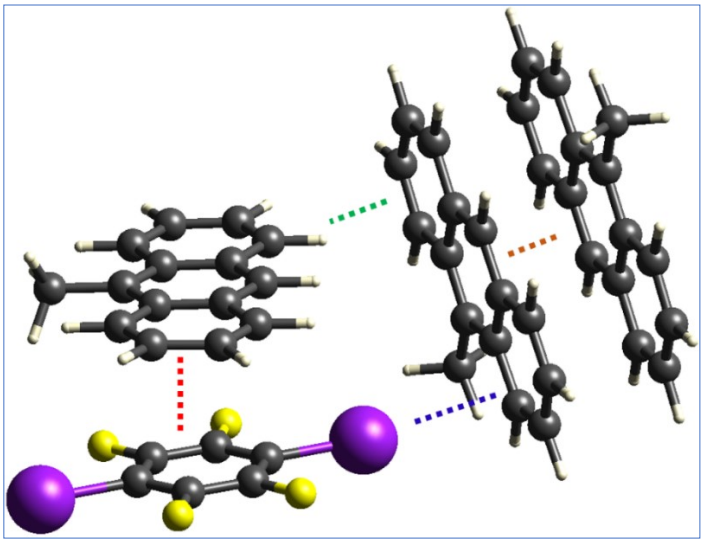

Figure ESI-16. Pairs of molecules contributing most to the total interaction energy in crystalline $(MA)_4$·I2F4

Table ESI-6. Electrostatic, polarization, dispersion, repulsion terms and total interaction energy within the pairs of molecules shown in Figure ESI-16. Evaluated with the Crystal Explorer Package and using the CE-HF/3-21G (k_ele = 1.019; k_pol = 0.651; k_disp =0.901; k_rep = 0.811) as energy model and basis set.[4-6]

Interaction	$E_{ELECTROSTATIC}$	$E_{POLARIZATION}$	$E_{DISPERSION}$	$E_{REPUSLSION}$	E_{TOTAL}
	-13.1	-3.6	-59.0	26.5	-47.4
	-12.1	-2.5	-21.6	19.5	-17.6
	-5.9	-1.7	-20.4	9.4	-17.9
	3.5	-7.7	-73.5	36.0	-38.5

References

1 A. F. Mabied, M. Müller, R. E. Dinnebier, S. Nozawa, M. Hoshino, A. Tomita, T. Sato and S. Adachi, *Acta Crystallogr. B.*, 2012, **68**, 424–430.

2 J. Dey and I. M. Warner, *J. Phys. Chem. A*, 1997, **101**, 4872–4878.

3 T. Hinoue, Y. Shigenoi, M. Sugino, Y. Mizobe, I. Hisaki, M. Miyata and N. Tohnai, *Chem. – A Eur. J.*, 2012, **18**, 4634–4643.

4 P. R. Spackman, M. J. Turner, J. J. McKinnon, S. K. Wolff, D. J. Grimwood, D. Jayatilaka and M. A. Spackman, *J. Appl. Crystallogr.*, 2021, **54**, 1006–1011.

5 C. F. Mackenzie, P. R. Spackman, D. Jayatilaka and M. A. Spackman, *IUCrJ*, 2017, **4**, 575–587.

6 S. P. Thomas, P. R. Spackman, D. Jayatilaka and M. A. Spackman, *J. Chem. Theory Comput.*, 2018, **14**, 1614–1623.